Bioelectrochemistry 75 (2009) 44–49

Contents lists available at ScienceDirect

Bioelectrochemistry

journal homepage: www.elsevier.com/locate/bioelechem

A novel tyrosinase biosensor based on biofunctional ZnO nanorod microarrays on the nanocrystalline diamond electrode for detection of phenolic compounds

Jianwen Zhao [a,*], Daohong Wu [a], Jinfang Zhi [b]

[a] College of Chemistry and Chemical Engineering, Jishou University, Jishou, Hunan Province, 416000, PR China
[b] Laboratory of Organic Optoelectronic Functional Materials and Molecular Engineering, Technical Institute of Physics and Chemistry & Graduate university of Chinese Academy of Sciences, No.2, Beiyitiao, Zhong-guan-cun, Haidian District, Beijing, 100080, PR China

ARTICLE INFO

Article history:
Received 3 November 2008
Received in revised form 12 January 2009
Accepted 18 January 2009
Available online 3 February 2009

Keywords:
Tyrosinase
Boron-doped nanocrystalline diamond thin film
Biofunctional ZnO nanorod microarrays
Phenolic compounds

ABSTRACT

A novel tyrosinase biosensor based on biofuncational ZnO nanorod microarrays on the boron-doped nanocrystalline diamond (BDND) substrates was developed. The ZnO nanorod microarrays were firstly deposited on BDND thin film surfaces via a low-temperature solution method, and then ZnO nanorods were functionalized with the mixture of 3-aminopropyltriethoxysilane (APTES) and tetraethoxysilane (TEOS) by a co-condensation approach, then tyrosinase was immobilized to amino-modification ZnO nanorod surfaces by the covalent binding. As-prepared tyrosinase biosensors were used for the detection of phenolic compounds. The tyrosinase-modified BDND electrode gave a linear response range of 1–175, 1–150 and 1–150 μM and sensitivity of 576.2, 339.3 and 287.1 μA $mmol^{-1}$ cm^{-2} for *p*-cresol, 4-chlorophenol and phenol, respectively. The low detection limit was estimated to be 0.1, 0.25 and 0.2 μM ($s_b/m=3$), respectively. Therefore, the biofunctional ZnO nanorod arrays have potential applications as platforms to immobilize other enzymes and bioactive molecules in biosensors.

1. Introduction

It is well-known that most of phenolic compounds show harmful effects on human health or the environment, so it is very important for us to develop the effective methods to quantitatively determine phenolic compounds. Amperometric tyrosinase biosensors have been extensively reported in the literature for the detection of various phenolic compounds due to its high sensitivity, effectiveness and simplicity. Generally, the immobilization of tyrosinase is a key step to fabricate the tyrosinase biosensor. At present, there have been developed many different methods to immobilize tyrosinase including the entrapment method [1,2], the noncovalent [3–11] and covalent methods [12–15]. However, some of them are relatively complex, or require the use of organic solvents, which lead to relatively poor stability and bioactivity of tyrosinase. Furthermore, the excellent electrode materials also play an important role in the development of high performance biosensor. Boron-doped nanocrystalline diamond (BDND) thin film is regarded as the third-generation biosensor support and the attractive new electrode materials because of biocompatibility and the good electrochemical properties including: wide electrochemical potential window, very low double-layer capacitance, extreme electrochemical stability and high resistance to deactivation by fouling [16], and in most of these studies, the BDD thin film electrode has been demonstrated to be superior to the glass carbon (GC) electrode and other electrodes in terms of high signal-to-noise ratio, long-term stability, high sensitivity, and good reproducibility. Thus, the BDND thin film electrodes are of interest for a variety of electrically based chemical and biological sensing applications [17]. However, the as-deposited diamond thin film electrode surface is hydrogen-terminated, and biomolecules can not be directly immobilized on it. For the realization of biosensors based on the diamond thin film, bonded linker molecular layers are required. Recent studies have shown that the functionalization of diamond film can serve as a starting point for preparing biomolecular interfaces, which exhibit excellent biomolecular recognition properties [18–22]. However, the introduction of functional groups was rather limited via the chemical methods, and the as-prepared biosensors resulted in a low sensitivity and high detect limit. Furthermore, some biosensors retained its initial sensitivity only for a few days in storage under dry condition due to weaker bonding of functional molecular with BDD surface [14]. Moreover, diamond thin films can not be reused after modification by chemical methods.

Being a key functional material with versatile properties, ZnO nanostructures such as nanowires, nanotips and nanorods have received more and more attention in the biosensor applications due to its distinguished performance [23–32]. Firstly, ZnO nanomaterial is a biocompatible material with a high isoelectric point (IEP) of about 9.5, which make it suitable for absorption of proteins with low IEPs, as the protein immobilization is primarily driven by electrostatic interaction. Secondly, ZnO nanostructures have unique advantages including the high specific surface area, nontoxicity, chemical stability,

* Corresponding author. Tel./fax: +86 743 8563911.
E-mail address: zhjw76@hotmail.com (J. Zhao).

1567-5394/$ – see front matter
doi:10.1016/j.bioelechem.2009.01.005

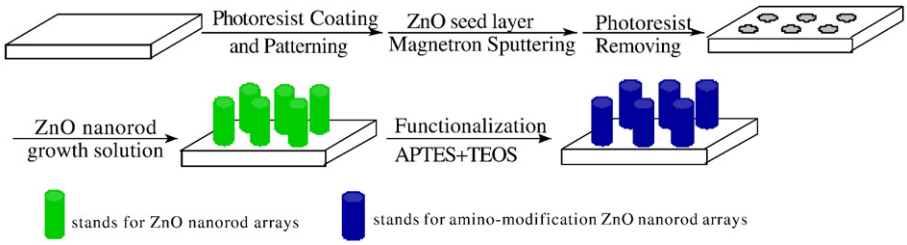

Scheme 1. Schematic protocol for the fabrication processes of amino-modification ZnO nanorod microarrays on BDND thin film surfaces.

electrochemical activity, and high electron communication features. Thirdly, they can be easily prepared through chemical solution processes including sol–gel, hydrothermal synthesis and electrochemical deposition. Hence, different biosensors based on ZnO nanomaterials have been widely developed [3–9], such as glucose sensor, tyrosinase sensor, uric acid biosensor, horseradish peroxidase biosensor, DNA biosensor and so on. However, these biosensors have some disadvantages, such as instability and nonspecificity, which is due to the weak interaction between ZnO nanomaterials and biomolecules. Although there have been a few reports about depositing ZnO films on diamond surfaces including radio frequency magnetron sputtering, chemical vapor deposition and electrochemical deposition, and it has been widely used in the field emission display, ultraviolet photodetector and surface acoustic wave (SAW), the fabrication of micropatterned ZnO nanostructures onto the diamond thin film substrates and the development of a covalently bonded enzyme biosensor have seldom been reported.

Here we described a new tyrosinase biosensor based on the covalent immobilization of tyrosinase on biofunctional ZnO nanorod microarrays on the BDND thin film electrode. The morphologies and components of ZnO nanorods before and after modification were characterized by scanning electron microscopy (SEM), transmission electron microscopy (TEM) and X-ray photoelectron spectroscopy (XPS). The response dependences and amperometric characteristics of the prepared enzyme electrode in the detection of phenolic compounds was investigated. The results showed that the developed biosensor exhibited good stability and high sensitivity for the detection of phenolic compounds.

2. Experimental

2.1. Chemicals and reagents

Tyrosinase (EC 1.14.18.1, 3216 U mg^{-1} from mushroom) was purchased from Fluka (packed in Switzerland). 4-Chlorophenol, phenol and *p*-cresol were obtained from Wako Chemical Co. (Japan). 3-aminopropyltriethoxysilane (APTES) and tetraethoxysilane (TEOS) were purchased from Sigma. Glutaraldehyde (GA, 25% water solution) and BP212 positive photoresist were purchased from Aldrich and Beijing Institute of Chemical Reagent, respectively. The water used throughout this work was ultrapure water (18 MΩ cm) produced by Millipore Milli Q system. All of the chemical reagents were used as received without further purification.

2.2. Instrumentation

The BDND thin film was deposited on n-Si (111) wafers using hot filament chemical vapor deposition (HFCVD) apparatus (made by Shanghai Jiaotong University, P. R. China). The scanning electron microscope (SEM) images were taken using a Hitachi Ultra-high-Resolution S-4800 scanning electron microscope. Transmission electron microscopy (TEM) was done by an FEI Philips Tecnai 20 Electron Microscope. X-ray photoelectron spectroscopy (XPS) analysis was used Al Kα radiation in an ESCA Lab 220I-XL instrument. ZnO buffer layer was deposited on the BDND substrate in a JPGF-450 model radio frequency magnetron sputtering system with a base pressure of 2×10^{-3} Pa. Raman spectrum was obtained using Renishaw 1000 Raman spectrometer (Renishaw LTD., UK).

2.3. Fabrication of ZnO nanorod arrays

The non-micropatterned ZnO nanorod arrays were constructed according to precious report [33]. The ZnO seed layer was firstly deposited on the BDND thin film surface using a sol–gel method, then the BDND substrates were placed into in the solutions containing an equimolar (0.025 M) aqueous solution of zinc nitrate hexahydrate and hexamethylenetetramine and reacted at 65 °C for 6 h. The ZnO nanorod microarrays were fabricated by a photolithography process and the fabrication process was shown in Scheme 1. The BP212 positive photoresist was firstly spin-coated onto the BDND thin film surface, and then Cu-grids were covered onto the photoresist coated

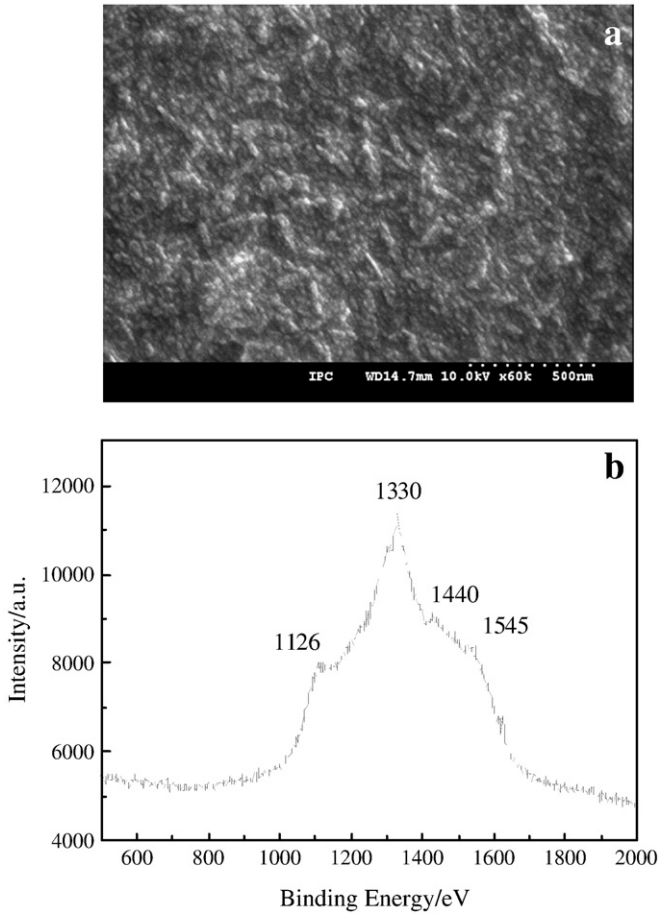

Fig. 1. The SEM image and Raman spectrum of as-prepared BDND thin film. (a) SEM image and (b) Raman spectrum.

BDND thin film surface as a mask and exposed to 365 nm UV light for 3 min. The exposed photoresist was developed with 0.5% (w/w) sodium hydroxide solution to remove the photoresist, and then baked at 100 °C for another 10 min, then the ZnO buffer layer was deposited on the BDND thin film surface by radio-frequency magnetron sputtering system for 10 min. The remanent photoresist was then removed through rinsing with acetone. The ZnO nanorod microarrays were obtained by placing the pre-micropatterned BDND substrates in the ZnO nanorod growth solutions and reacted at 65 °C for 6 h.

2.4. Preparation of amine-modification ZnO nanorod arrays

The process for preparation of amine-modification ZnO nanorod arrays was carried out as follows. Firstly, physically absorbed ZnO particles on the ZnO nanorod microarrays were removed by sonication the samples in ultrapure water for 15 min, then the ZnO nanorod microarrays were placed in the mixture of ethanol (30 mL), deionized water (2.5 mL), aqueous ammonia (1.5 mL), TEOS (100 μL) and APTES (100 μL) [29,30], and then solution was stirred by a magnetic stir bar for 3 h. After the coating reaction, the functionalized ZnO nanorod arrays were sonicated in ultrapure water again for 5 min. The samples were analyzed by XPS and TEM.

2.5. Immobilization of tyrosinase on amine-functionalized ZnO nanorod microarrays

Tyrosinase was immobilized onto amine-functionalized ZnO nanorod arrays by GA and the detailed process was as follows. The amine-modification ZnO nanorod microarrays were treated with the 2.5% GA solution for 2 h at room temperature in a shaking condition and washed three times with deionized water, and then 10 μL of 20 mg L^{-1} tyrosinase solution was dropped onto the surface of the electrode surface and the electrode was storied overnight at 4 °C so that the tyrosinase could be sufficiently immobilized onto the surface of the amine-modification ZnO nanorod arrays. Finally, the tyrosinase biosensor was successfully constructed.

2.6. Electrochemical measurements

Voltammetric and amperometric measurements were carried out with a potentiostat/galvanostat (Princeton 263A) in a three-electrode cell system. As-prepared tyrosinase electrode was used as a working electrode with an area of about 0.10 cm^2. A saturated calomel reference electrode (SCE) and a Pt stick counter electrode were also employed. Cyclic voltammetric and amperometric measurements were carried out in a 50 mL electrochemical cell. Cyclic voltammetry (CV) was typically performed at a scan rate of 25 mV s^{-1}. Unless otherwise stated, all experiments were carried out at room temperature in phosphate buffer solution (PBS) (0.1 M, pH 7).

3. Results and discussion

3.1. Characterization of BDND thin film electrode

Fig. 1 showed the SEM image and the Raman spectra of as-prepared BDND thin film electrode. As was shown in Fig. 1a, the grain size of BDND thin film obtained by HFCVD was about 20–30 nm. The intense wide peaks 1330 cm^{-1} is assigned to crystalline sp^3-hybridized carbon Raman peak (Fig. 1b). Broadening of the diamond band is a result of decreasing the grain size to the nanometer scale [34]. The presence of scattering peak at 1545 cm^{-1} is due to increasing graphite-like sp^2 bonded components at the grain boundaries in films,

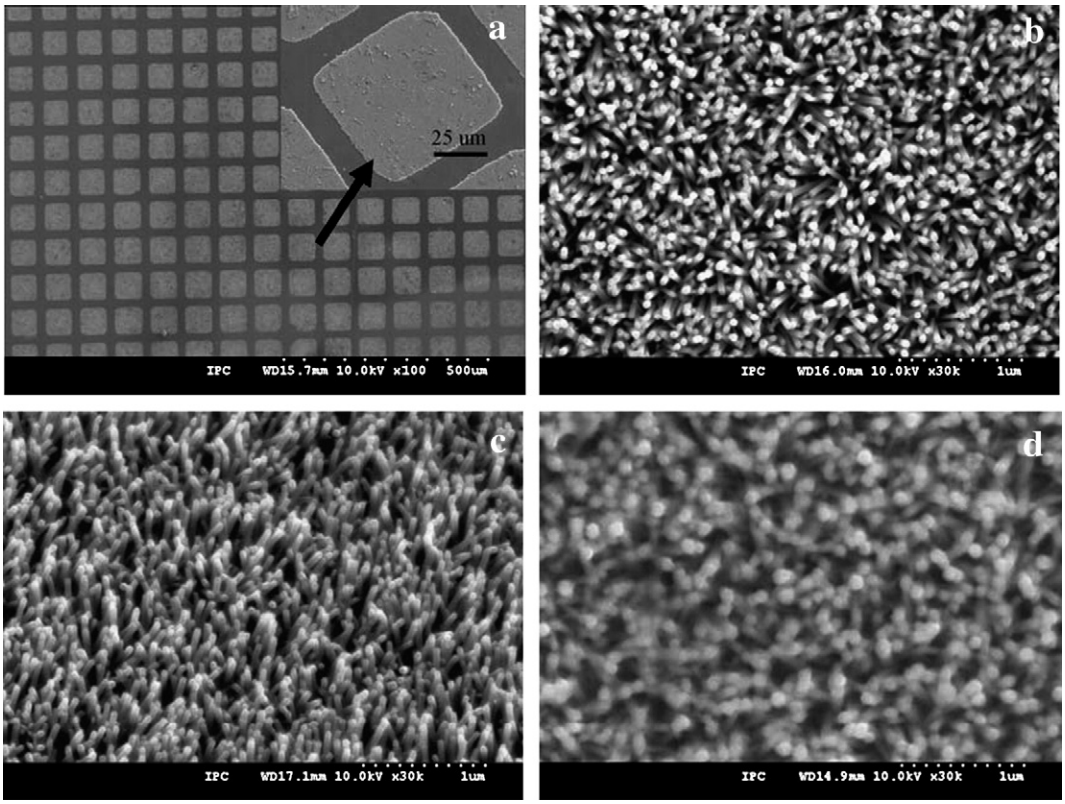

Fig. 2. SEM images of (a) the ZnO nanorod microarrays on BDND thin film surfaces (the inset shows the SEM image of a square-shape ZnO nanorod array), (b) top view of ZnO nanorod arrays, (c) tilt view of ZnO nanorod arrays and (d) functional ZnO nanorod arrays.

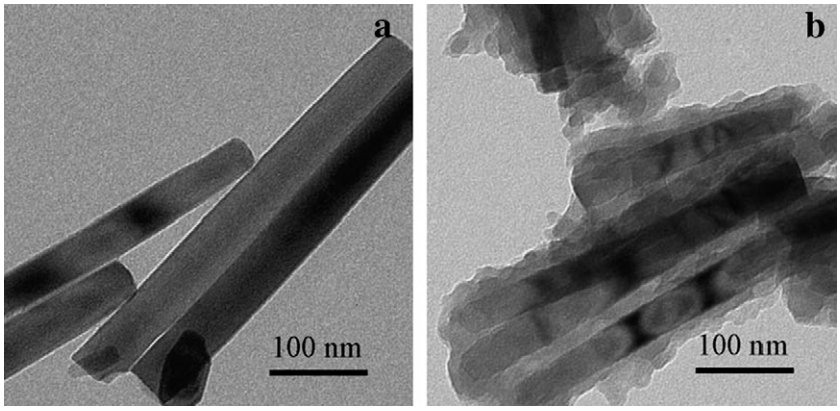

Fig. 3. TEM images of ZnO nanorods (a) before and (b) after modification with the mixture of TEOS and APTES.

and two scattering peaks at 1126 cm^{-1} and 1440 cm^{-1} are attributed to BDND Raman peaks [35].

3.2. Characteristics of amine-functional ZnO nanorod microarrays

The morphologies of ZnO nanorods and amine-functional ZnO nanorods were observed by SEM and TEM. Fig. 2a represented the preparation of the ZnO nanorod microarrays on the BDND thin film surface. It could be seen from Fig. 2a that the edges of micropattern lines were almost straight and uniform. Fig. 2b and c showed the top view and tilt view of ZnO nanorod arrays grown on the BDND substrates and the diameter of ZnO nanorod was about 50 nm. After modification with the silica by a co-condensation process (a mixture of TEOS and APTES), the SEM image of ZnO nanorods became blurry because of the non-conductive silica coatings (Fig. 2d). Furthermore, in order to ascertain the structure of the prepared nanocomposites, TEM image was performed. Representative TEM images were shown in Fig. 3, it could be seen that there were an inhomogeneous silica coating out of ZnO nanorod after modification. Furthermore, a comparison of XPS spectra recorded from the bare ZnO and amine-functional ZnO nanorods were shown in Fig. 4. It could be seen from Fig. 4 that the N 1s, Si 2s and Si 2p peaks were observed at 400.3 eV, 154.2 eV and 103.2 eV, respectively. In conclusion, the above results sufficiently demonstrated that amine-modification ZnO nanorod arrays were obtained on the BDND thin film surfaces after modification with the mixture of TEOS and APTES.

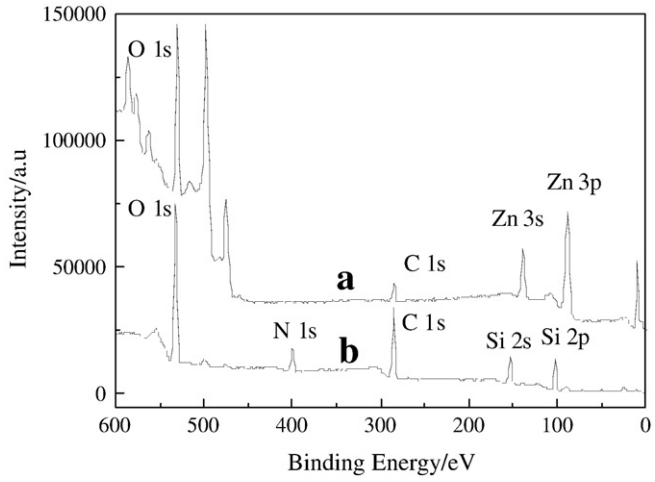

Fig. 4. XPS spectra of ZnO nanorods (a) before and (b) after functionalization.

3.3. CV curves for phenolic compounds at the tyrosinase electrode

Fig. 5 shows the typical CV curves of the tyrosinase modified electrode in the presence and absence of *p*-cresol in 0.1 M PBS (pH 7). In the absence of *p*-cresol, only a low background current was observed, after adding *p*-cresol to the PBS, the CV curves gave a well-defined peak locating at −0.12 V, which was due to the reduction of o-quinone species liberated from the enzymatic reaction on the electrode surface. Furthermore, the reduction peak currents increased with increasing the concentration of *p*-cresol. It demonstrated that the tyrosinase enzyme could retain its bioactivity to a large extent when being immobilized on biofunctional ZnO nanorod arrays by the covalent binding.

3.4. Effects of pH and applied potential

The enzyme activities were seriously affected by the buffer solution pH value, so the effect of the pH value of buffer solution was investigated in the range from 5.5 to 8.5. The results showed that the maximum current response was obtained at the pH value of 7, so a pH of 7 for the PBS was selected for the following experiments. The effect of applied potential for the tyrosinase biosensor on the amperometric signal and background current is also investigated. When the applied potential was −0.15 V (vs. SCE), the enzyme electrode displayed the larger current response to *p*-cresol and low background current.

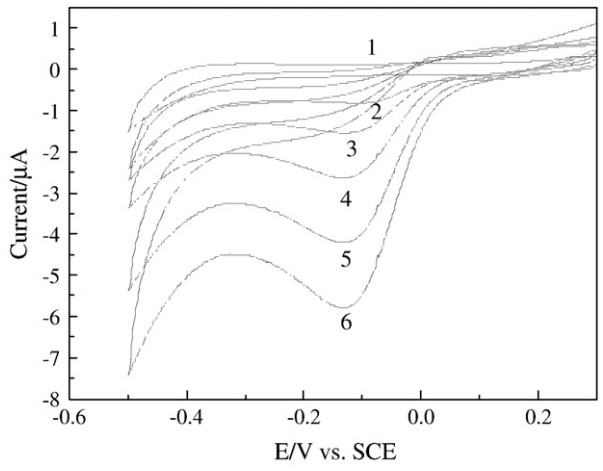

Fig. 5. Typical CV curves of *p*-cresol on as-prepared tyrosinase electrode. (1) blank, (2) 5 μM, (3) 25 μM, (4) 50 μM, (5) 75 μM and (6) 100 μM *p*-cresol, respectively. (The supporting electrolyte is 0.1 M PBS solution; the scan rate and the work electrode area are 25 mV s^{-1} and 0.1 cm^2, respectively.)

Therefore, the potential of −0.15 V (vs. SCE) was regarded as the optimum potential for the amperometric measurements.

3.5. Amperometric response of the tyronsinase modified BDND thin film electrode

The performance of biosensor was evaluated by testing the tyronsinase modified BDND thin film electrode in phenolic compounds with increased concentrations. Fig. 6a showed a typical amperometric response for the tyronsinase modified electrode at −0.15 V (vs. SCE) after the addition of successive aliquots of *p*-cresol, 4-chlorophenol and phenol to the 0.1 M PBS (pH 7) under constant stirring. A well-defined reduction current proportional to the concentration of *p*-cresol, 4-chlorophenol and phenol were observed. Fig. 6b showed the typical calibration curve of the tyronsinase electrode to *p*-cresol, 4-chlorophenol and phenol, respectively. The characteristics of the tyronsinase electrode to *p*-cresol, 4-chlorophenol and phenol including sensitivity, linear range and detection limit were listed in Table 1. As were shown in Table 1. The sensitivities of the prepared tyronsinase biosensor were 576.2, 339.3 and 287.1 μA $mmol^{-1}$ cm^{-2} for *p*-cresol, 4-chlorophenol and phenol, respectively, and it was higher than other tyrosinase biosensors [10–11,14], which could be attributed to the biocompatible microenvironment for the enzyme provided by the ZnO/BDND electrode and the high loading of enzyme by the development method. As tyrosinase had different affinity towards its substrates, each phenolic compound has different sensitivity, and sensitivities follow the order as: *p*-cresol> 4-chlorophenol>phenol, which was consistent with the previous reports [14,15]. The detection limits were also calculated according to the formula $3s_b/m$ criteria, where s_b and m were the standard deviation of the background current and the slope of the calibration graph, respectively. The detection limits were 0.1, 0.2 and 0.25 μM for *p*-cresol, 4-cholorophenol and phenol, respectively, under present experimental condition, which was slightly higher than other reports [14]. Furthermore, the developed enzyme electrode showed good reproducibility. The relative standard deviation (RSD) estimated by 15 successive measurements of 50 μM *p*-cresol solution at −0.15 V (vs. SCE) was about 2.1%. For different batches of enzyme electrodes, prepared under the same condition, the acceptable reproducibility was obtained with a coefficient of 3.1% for the current response to the same sample at −0.15 V (vs. SCE). Furthermore, compared with the photochemical method and the diazonium method as described in Refs. [14,15,17–21], the proposed method had another distinct advantage, i.e., the BDND thin film electrode could be reused repeatedly.

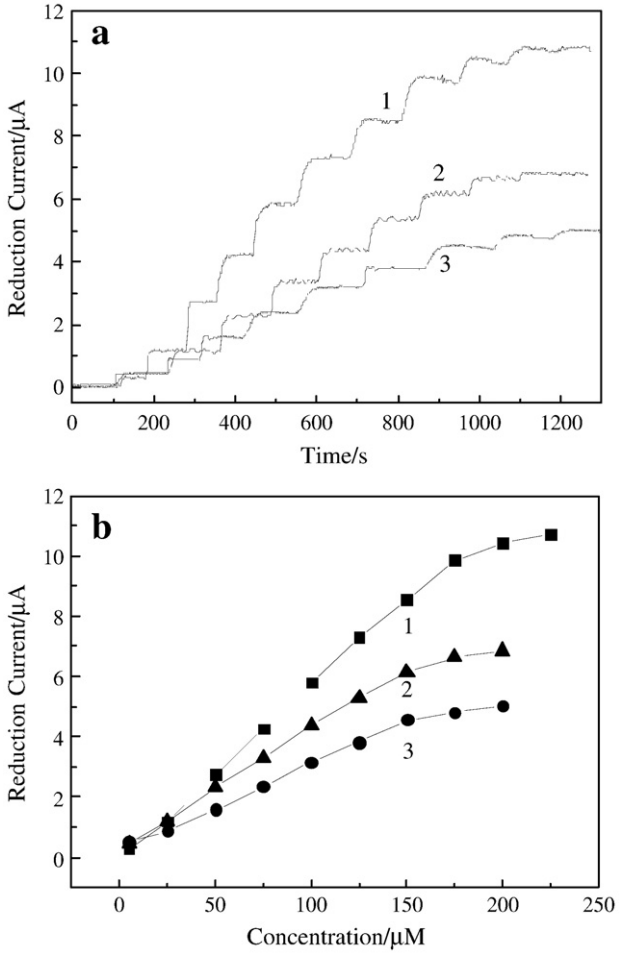

Fig. 6. (a) Typical amperometric response of the as-prepared tyrosinase biosensor to different phenolic compounds in 0.1 M PBS solution (pH=7) (Applied potential is −0.15 V vs. SCE, and the work electrode area is 0.1 cm^2), (b) the calibration curves between the reduction current and the concentration of different phenolic compounds. (1) *p*-cresol, (2) 4-chlorophenol and (3) phenol, respectively.

Table 1
Response characteristics of the tyronsinase biosensor to phenolic compounds

Analyte	Sensitivity (μA $mmol^{-1}$ cm^{-2})	Linear range (μM)	Limit of detection (μM)	*R*
p-cresol	576.2	1–175	0.1	0.999
4-Chlorophenol	339.3	1–150	0.2	0.999
Phenol	287.1	1–150	0.25	0.998

R represents as the correlation coefficient of the linear range.

3.6. Stability of the tyronsinase electrode

The stability of the tyronsinase electrode was also studied. The biosensors were stored dry at 4 °C and their response to 50 μM *p*-cresol was measured in 0.1 M PBS (pH 7) at −0.15 V (vs. SCE) every other day. The prepared enzyme electrode retained about 90% of its initial activity after 3 weeks and the response decreased to about 80% of the initial value after 5 weeks. The decrease in sensitivity was possibly due to the leakage of enzyme during the electrochemical measurement, at the same time, the activity of enzyme might also be decreasing with time.

As control experiments, tyrosinase was also immobilized on bare micropatterned and non-micropatterned ZnO nanorod arrays by electrostatic force. No obvious current response was observed on non-micropatterned ZnO nanorod array modified electrode within the potential window, which was attributed to the density ZnO film inhibit electron transport. When tyrosinase was directly adsorbed on the surface of bare micropatterned ZnO nanorod arrays, the prepared enzyme electrode could give a high current response, however, the reduction peak current decreased gradually with increasing the scan times because of the weak binding forces between tyrosinase and ZnO nanorod.

4. Conclusions

The tyrosinase biosensor has been developed based on biofunctional ZnO nanorod microarrays on BDND thin film electrode. The resulted enzyme electrode exhibited high sensitivity and stability for the amperometric detection of phenolic compounds. It may be extended to other enzymes and other bioactive molecules, and the possible application of this kind of biosensor maybe focused on environmental and industrial monitoring. Furthermore, the ZnO nanorod microarrays grown on the nanocrystalline diamond substrate have a potential application in field emission and electroluminescent devices.

Acknowledgements

This work was supported by the National Natural Science Foundation of China (20773150).

References

[1] G. Wang, J.J. Xu, L.H. Ye, J.J. Zhu, H.Y. Chen, Highly sensitive sensors based on the immobilization of tyrosinase in chitosan, Bioelectrochemistry 57 (2002) 33–38.

[2] E. Dempsey, D. Diamond, A. Collier, Development of a biosensor for endocrine disrupting compounds based on tyrosinase entrapped within a poly(thionine) film, Biosens. Bioelectron. 20 (2004) 367–377.

[3] C.L. Zhang, M.C. Liu, P. Li, Y.Z. Xian, Y.X. Cheng, Fabrication of ZnO nanorod modified electrode and its application to the direct electrochemical determination of hemoglobin and cytochrome c, Chin. J. Chem. 23 (2005) 144–148.

[4] E. Topoglidis, A.E. G Cass, B. O'Regan, J.F. Durrant, Immobilisation and bioelectrochemistry of proteins on nanoporous TiO_2 and ZnO films, J. Electroanal. Chem. 517 (2001) 20–27.

[5] J.F. Zang, C.M. Li, X.Q. Cui, J.X. Wang, X.W. Sun, H. Dong, C.Q. Sun, Tailoring zinc oxide nanowires for high performance amperometric glucose sensor, Electroanalysis 19 (2007) 1008–1014.

[6] Z.W. Zhao, X.J. Chen, B.K. Tay, J.S. Chen, Z.J. Han, K.A. Khor, A novel amperometric biosensor based on ZnO:Co nanoclusters for biosensing glucose, Biosens. Bioelectron. 23 (2007) 135–139.

[7] F.F. Zhang, X.L. Wang, S.Y. Ai, Z.D. Sun, Q. Wan, Z.Q. Zhu, Y.Z. Xian, L.T. Jin, K. Yamamoto, Immobilization of uricase on ZnO nanorods for a reagentless uric acid biosensor, Anal. Chim. Acta 519 (2004) 155–160.

[8] Z.M. Liu, Y.L. Liu, H.F. Yang, Y. Yang, G.L. Shen, R.Q. Yu, A mediator-free tyrosinase biosensor based on ZnO sol–gel matrix, Electroanalysis 17 (2005) 1065–1070.

[9] Y.F. Li, Z.M. Liu, Y.L. Liu, Y.H. Yang, G.L. Shen, R.Q. Yu, A mediator-free phenol biosensor based on immobilizing tyrosinase to ZnO nanoparticles, Anal. Biochem. 349 (2006) 33–40.

[10] V.C. Sanz, M.L. Mena, J.M. Pingarron, Development of a tyrosinase biosensor based on gold nanoparticles-modified glassy carbon electrodes: application to the measurement of a bioelectrochemical polyphenols index in wines, Anal. Chim. Acta 528 (2005) 1–8.

[11] B. Wang, J. Zhang, S. Dong, Silica sol–gel composite film as an encapsulation matrix for the construction of an amperometric tyrosinase-based biosensor, Biosens. Bioelectron. 15 (2005) 397–402.

[12] K. Rajesh, W. Takashima, K. Kaneto, Amperometric phenol biosensor based on covalent immobilization of tyrosinase onto an electrochemically prepared novel copolymer poly(N-3-aminopropyl pyrrole–copyrrole) film, Sens. Actuat. B. 102 (2004) 271–277.

[13] T. Mai Anh, S.V. Dzyadevych, A.P. Soldatkin, N.D. Chien, N. Jaffrezic-Renault, J.M. Chovelon, Development of tyrosinase biosensor based on pH-sensitive field-effect transistors for phenols determination in water solutions, Talanta 56 (2002) 627–634.

[14] Y.L. Zhou, R.H. Tian, J.F. Zhi, Amperometric biosensor based on tyrosinase immobilized on a BDD electrode, Biosens. Bioelectron. 22 (2007) 822–828.

[15] Y.L. Zhou, J.F. Zhi, Development of an amperometric biosensor based on covalent immobilization of tyrosinase on a boron-doped diamond electrode, Electrochem. Comm. 8 (2006) 1811–1816.

[16] A. Fujishima, Y. Einaga, T.N. Rao, Diamond Electrochemistry, First Edition, Elsevier, 2005, pp. 28–31.

[17] R.R. Jorge, H. Jorge, L.R. Beatriz, H. Andreas, S. Doris, S. Martin, L.C. Enrique, A.G. José, Synthetic nanocrystalline diamond as a third-generation biosensor support, Langmuir 22 (2006) 5837–5842.

[18] T. Knickerbocker, T. Strother, M.P. Schwartz, J.N. Russell Jr., J. Butler, L.M. Smith, R.J. Hamers, DNA-modified diamond surfaces, Langmuir 19 (2003) 1938–1942.

[19] W. Yang, O. Auciello, J.E. Butler, W. Cai, J.A. Carlisle, J.E. Gerbi, D. Gruen, T. Knickerbocker, T.L. Lasseter, J.N. Russell, L.M. Smith, R.J. Hamers, DNA-modified nanocrystalline diamond thin films as stable, biologically active substrates, Nature Materials 1 (2002) 253–257.

[20] G.J. Zhang, K.S. Song, Y. Nakamura, T. Ueno, T. Funatsu, I. Ohdomari, H. Kawarada, DNA micropatterning on polycrystalline diamond via one-step direct amination, Langmuir 22 (2006) 3728–3734.

[21] M.C. Granger, M. Mermoux, J.W. Strojek, G.M. Swain, Standard electrochemical behavior of high-quality boron-doped polycrystalline diamond thin-film electrodes, Anal. Chem. 72 (2000) 3793–3804.

[22] J.K. Luo, Y.Q. Fu, H.R. Le, J.A. Williams, S.M. Spearing, W.I. Milne, Diamond and diamond-like carbon MEMS, J. Micromech. Microeng. 17 (2007) S147–S163.

[23] J.X. Wang, X.W. Sun, A. Wei, Y. Lei, Zinc oxide nanocomb biosensor for glucose detection, Appl. Phys. Lett. 88 (2006) 233106–233108.

[24] A. Wei, X.W. Sun, J.X. Wang, Enzymatic glucose biosensor based on ZnO nanorod array grown by hydrothermal decomposition, Appl. Phys. Lett. 89 (2006) 123902–123904.

[25] Y.L. Liu, Y.H. Yang, H.F. Yang, Z.M. Liu, G.L. Shen, R.Q. Yu, Nanosized flower-like ZnO synthesized by a simple hydrothermal method and applied as matrix for horseradish peroxidase immobilization for electro-biosensing, J. Inorg. Biochem. 99 (2005) 2046–2053.

[26] N. Kumar, A. Dorfman, J.I. Hahm, Ultrasensitive DNA sequence detection using nanoscale ZnO sensor arrays, Nanotechnology 17 (2006) 2875–2881.

[27] N. Kumar, A. Dorfman, J.I. Hahm, Highly sensitive biomolecular fluorescence detection using nanoscale ZnO platforms, Langmuir 22 (2006) 4890–4895.

[28] T.Y. Liu, H.C. Liao, C.C. Lin, S. Hu, S.Y. Chen, Biofunctional ZnO nanorod arrays grown on flexible substrates, Langmuir 22 (2006) 5804–5809.

[29] L. Nie, L. Gao, P. Feng, J. Zhang, X. Fu, Y. Liu, T. Wang, Three-dimensional functionalized tetrapod-like ZnO nanostructures for plasmid DNA delivery, Small 2 (2006) 621–625.

[30] L. Nie, L.Z. Gao, X.Y. Yan, T.H. Wang, Functionalized tetrapod-like ZnO nanostructures for plasmid DNA purification, polymerase chain reaction and delivery, Nanotechnology 18 (2007) 015101–015106.

[31] R. Yakimova, G. Steinhoff, R.M. Petoral Jr., C. Vahlberg, V. Khranovskyy, G.R. Yazdi, K. Uvdal, A. Lloyd Spetz, Novel material concepts of transducers for chemical and biosensors, Biosens. Bioelectron. 22 (2007) 2780–2785.

[32] J.W. Zhao, L.Z. Wu, J.F. Zhi, Fabrication of micropatterned ZnO/SiO_2 core/shell nanorod arrays on a nanocrystalline diamond film and their application to DNA hybridization detection, J. Mater. Chem. 18 (2008) 2459–2465.

[33] R. Kaur, A.V. Singh, R.M. Mehra, Sol–gel derived highly transparent and conducting Yttrium doped ZnO films, J. Non-Cryst. Solids. 352 (2006) 2335–2338.

[34] T. Xu, S.R. Yang, J.J. Lu, Q.J. Xue, J.Q. Li, W.T. Guo, Y.N. Sun, Characterization of nanocrystalline diamond films implanted with nitrogen ions, Diamond. Relat. Mater. 10 (2001) 1441–1447.

[35] Y.Q. Fu, B.B. Yan, N.L. Loh, Effects of pretreatment and interlayer on the nucleation and growth of diamond coatings on titanium substrate, Surf. Coating. Tech. 130 (2000) 173–185.